COVER SHEET

NOTE: This coversheet is intended for you to list your article title and author(s) name only

Paper Number: **To be Changed**

Title: **Progressive Damage and Failure Analysis of Bonded Composite Joints at High Energy Dynamic Impacts**

Authors: Akhil Bhasin
Suresh Raju Keshavanarayana
Luis Gomez
Aswini Kona Ravi
Brian P. Justusson
Gerardo Olivares

ABSTRACT

Both wing and fuselage structures utilize bonded composite joints for structural efficiency in modern commercial and military aircraft. To ensure compliance with certification requirements mechanical fasteners are typically used as a failsafe mechanism for appropriate strength in the event of complete stiffener disbond. However, the use of fasteners decreases the structural efficiency of the structure by adding weight. This establishes the requirement to better exploit the efficiency of bonded structures and fully understand the failure behavior of adhesively bonded composite structures, particularly when subjected to elevated loading rates due to high energy dynamic impacts (HEDI). For this reason, the NASA Advanced Composite Consortium (ACC) HEDI team developed an experimentation and numerical modeling program for high rate loading of composite joints [1] [2]. In the present work, the response of adhesively bonded composite joints subjected to elevated loading rates is studied numerically and validated against experimental results. Due to dynamic considerations of experiments, the idea of wedge insert [3] was extended to use with Split Hopkinson Pressure Bar (SHPB) testing techniques. Mode-I and Mode-II test configurations were simulated to evaluate the capability of two continuum damage material (CDM) models in LS-DYNA, namely MAT162 and MAT261 [4]. Three different levels of fidelity were considered to investigate the level of detail required to numerically predict the failure behavior and the results from high fidelity analysis are presented.

———————————

Akhil Bhasin, National Institute for Aviation Research, Wichita, KS 67260
S.R. Keshavanarayana, Aerospace Department at Wichita State University, Wichita, KS 67260
Luis Gomez, National Institute for Aviation Research, Wichita, KS 67260
Aswini Kona Ravi, National Institute for Aviation Research, Wichita, KS 67260
Brian P. Justusson, Boeing Research & Technology, St. Louis, MO 63134
Gerardo Olivares, National Institute for Aviation Research, Wichita, KS 67260

INTRODUCTION

There is an increasing desire to use bonded composite primary structures in commercial and military aircraft. The certification process requires demonstration of strength under a condition where a stringer completely disbonds and is typically addressed through the inclusion of fasteners at stringer terminations. This inclusion results in additional weight and reduces the structural efficiency. Since both wing and fuselage composite structures have a typical skin-stringer configuration, this requirement creates as a strong need for improved understanding of mechanical loading on composite structures. One particularly problem is under the impact of the outer mold line (OML). Even at relatively low impact energies, OML impacts opposite a flange can create significant stringer disbond [5]. The mechanics of disbond between the skin and stringer has not been adequately characterized, particularly under high energy dynamic impact (HEDI). Further, the response of these bonded structures under HEDI is not well understood due to the rapid evolution of delamination mode mixity as penetration events occur and the increase of strain rate effects becomes prominent.

In some co-cured structures (e.g. composites cured without an adhesive), the interface between the skin and stiffener consists solely of matrix. Under elevated loading rates, the material demonstrates brittle failure and higher strengths compared to quasi-static rates [5]. Thorsson et al. [3] studied the effect of dynamic crack propagation using a wedge insert fracture technique and showed that under higher loading rates, the Mode I fracture toughness decreases. However, the work noted that the higher loading rates such as those observed under HEDI were not achievable with the experimental setup. Noting the limitations, Ravindran et al [7] extended the approach through an analytical experimental design to ensure the same type of behavior across a range of higher loading rates. This same methodology was extended to a dynamic end notch flexure (ENF) test to study the loading rate effects on Mode II fracture.

The joints are loaded in the bounding cases of Mode-I and Mode-II test configurations with the use of modified SHPB [7] at impact velocities of 7.5 m/s, 10 m/s and 15 m/s. Test data measurement techniques included photogrammetry coupled with digital image correlation at a rate of one million frames per second and load data measurements from load cells. Post experimentation, numerical analysis was conducted using two commercially available, state-of-art Progressive Damage and Failure Analysis (PDFA) material models to evaluate the capabilities of current methodologies for simulating the dynamic behavior of bonded joints both quantitatively and qualitatively.

TECHNICAL APPROACH

Given the inherent multiscale nature of the problem, different engineering assumptions may be made to improve the fidelity of the modeling. The NASA ACC identified three modeling approaches to study:

1. Low Fidelity: The modelling approach assumes that the adhesive will not fail and that the dominant failure mode would be first ply failure and subsequent crack migration
2. Medium Fidelity: The modelling approach assumes that the adhesive may fail cohesively, but not adhesively while allowing for the first ply failure and crack migration to occur
3. High Fidelity: The modelling approach assumes that both adhesive and cohesive failure are possible while allowing first ply failure and crack migration to occur

The native LS-DYNA material models MAT162/MAT261 [4] were used for all three modelling behaviors to study the behavior of adhesively bonded composite joints subjected to elevated loading rates. This study focuses only on the results obtained from the high fidelity modelling approach, wherein the adhesive is modeled discretely using an elasto-plastic material model, and the interaction between composite-adhesive is defined using cohesive zone modeling as shown in Figure 1. Of note, different meshing techniques were employed based on program developed best practices, depending upon the type of material model used – orthogonal mesh for MAT162 and fiber aligned mesh for MAT 261.
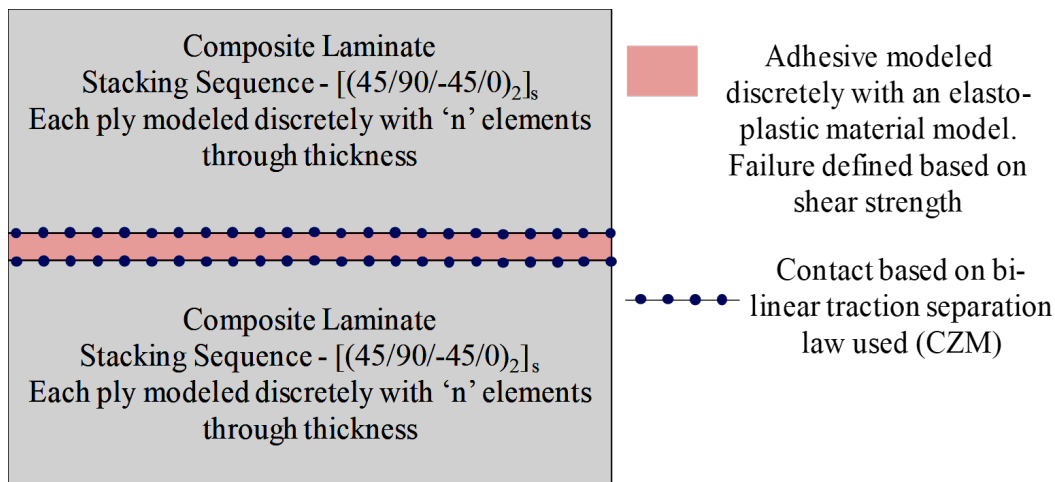

Figure 1 Schematic depicting numerical modeling methodology for high fidelity analysis

NUMERICAL MODELLING METHODOLOGY

The Finite Element (FE) models were generated conforming to the specimen and fixture dimensions as used in experimentation. Geometry, meshing methodologies, material properties and contact definitions adopted for both Mode-I and Mode-II configurations have been explained in this section.

Geometry and Meshing Methodologies

Both Mode-I and Mode-II failure in bonded joints were characterized using a modified SHPB [7] comprised of a striker bar, incident bar, load cells and fixtures instrumented to support the specimens. Given that the SHPB test setup is inherently a wave propagation based experimental procedure, a metal block was placed behind the specimen to reduce the effects of the reflected pulse. In order to generate a high fidelity numerical model and ensure that these wave propagations through multiple interfaces were accurately captured, the test-setup was modeled in detail for both the loading conditions as shown in Figure 2. A meso-level approach, wherein each ply is modeled explicitly, was implemented for both Mode-I and Mode-II specimens; however, meshing style varied depending on the type of material model used as shown in Figure 3 and Figure 4. Fiber-aligned mesh with one element through-thickness per ply was used for MAT261 models, whereas orthogonal mesh with varying elements through thickness per ply was used for MAT162 models.
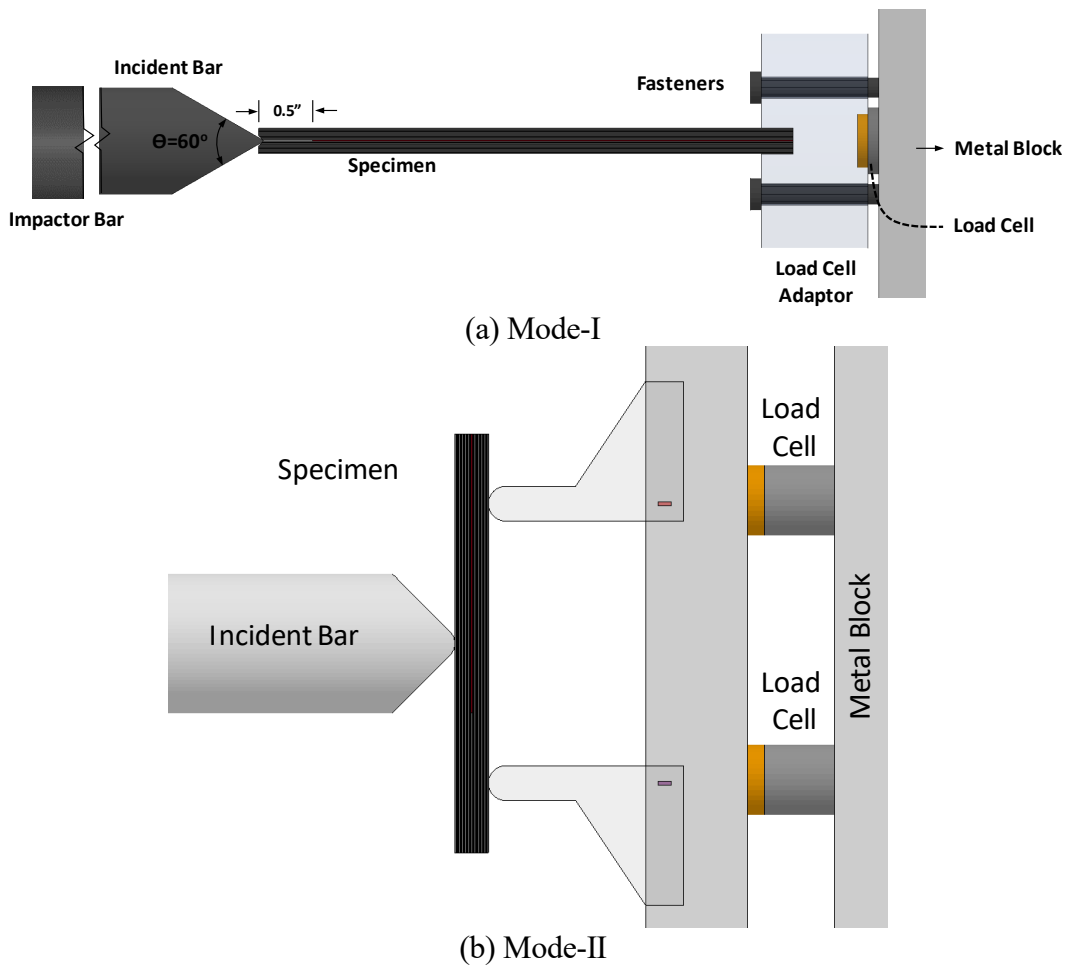

(a) Mode-I

(b) Mode-II

Figure 2 Finite Element (FE) models for (a) Mode-I and (b) Mode-II configurations
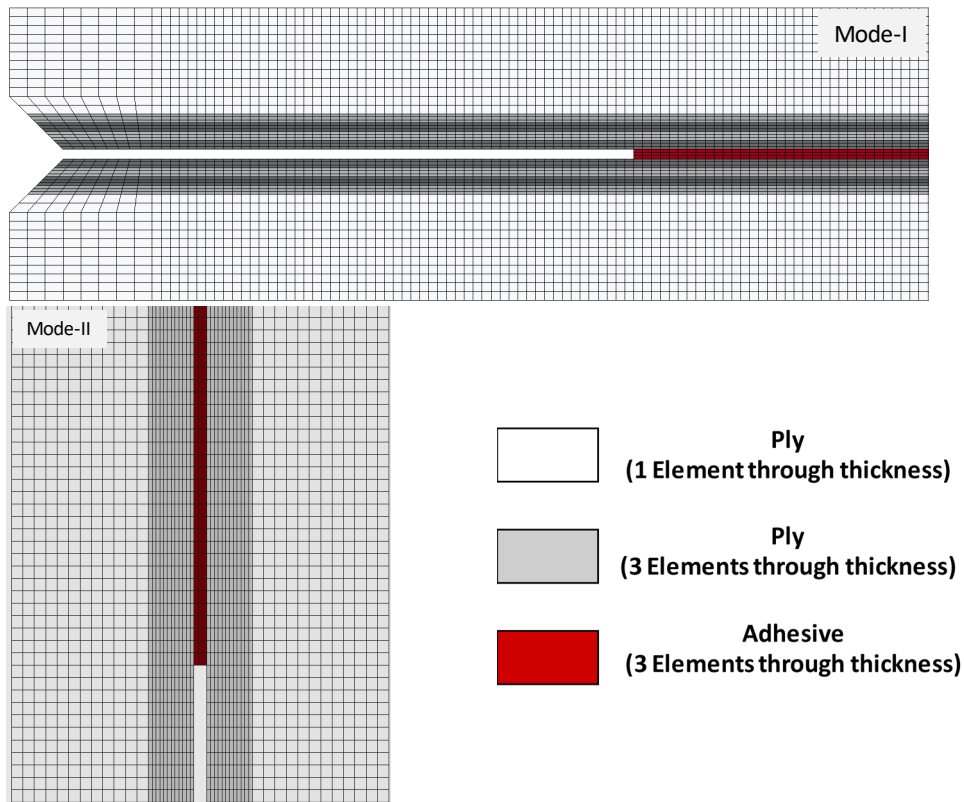
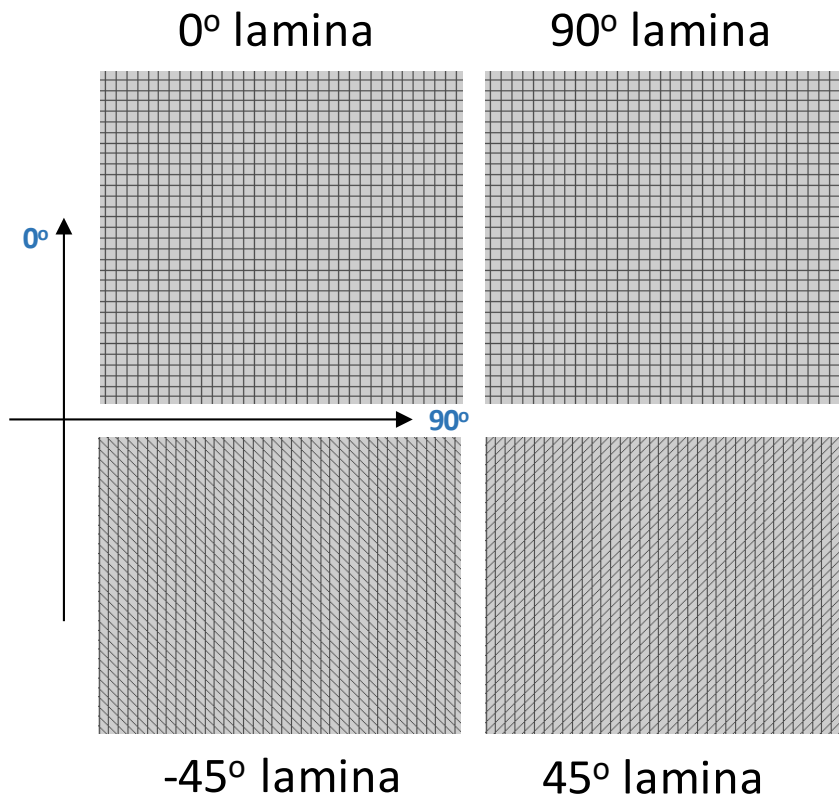Figure 3 Orthogonal meshing methodology for MAT162 models

Figure 4 Fiber aligned meshing methodology for MAT261 models

Material Properties

Specimens for both the loading conditions comprised of two Carbon Fiber Reinforced Polymer (CFRP) laminates (IM7/8552), each with sixteen plies, bonded with FM309-1 adhesive. The stacking sequence of the specimen was [(45/90/-45/0)$_{2S}$/Adhesive/(45/90/-45/0)$_{2S}$], with initial crack length of 0.5" and 1" for Mode-I and Mode-II respectively. Material properties for both the material models, MAT162 and MAT261, were extracted from 2CO3 – Deliverable 5.9.6 [8].

Incident bar, impactor bar and any other required fixture components were manufactured using Aluminum 6061-T6 and modeled using an elastic material model, MAT001. The material properties for the same were extracted from the Metallic Materials Properties and Standardization (MMPDS). Effective stiffness of load cell was calculated from the technical specification sheet and was also modeled using MAT001. An elasto-plastic material model, MAT024, was used to model adhesive with material properties available from 2C19 – Deliverable 4.9.32 [9].

Contact Properties

To capture delaminations within the laminate and to capture adhesive failure at the interface, an automatic single surface tiebreak contact was defined. This contact option uses Benzeggagh-Kenane mixed mode traction separation law with an option to define failure stresses and energy release rates under both Mode-I and Mode-II loading conditions. Fracture toughness values were determined from testing [9] and failure stress values were calibrated to match the load-displacement response of fracture toughness tests conducted at quasi-static loading conditions. An automatic surface to surface contact was defined at other interfaces.

Figure 5 Calibration of tiebreak contact based on quasi-static fracture toughness test results

RESULTS

Simulations were conducted at impact velocities of 7.5 m/s (the setup minimum velocity), 10 m/s and 15 m/s and were consistent with the velocities measured during testing. Both Mode I and Mode II test configurations were analyzed with the MAT162 and MAT261 material models using LS-DYNA R8 solver on double precision. The memory system used was Symmetrical Multiprocessing (SMP) and after an internal study of CPU efficiency, 20 cores were used for each run. Consistent with best practices for modelling dynamic events, mass scaling and damping were not used during these studies.

Sprague and Geers' (S&G) error metric [10] was used to evaluate the accuracy of both MAT162 and MAT261 material models in predicting the load response obtained from experiments. S&G error metric was selected because it calculates magnitude and phase error separately by using Equation 1 and Equation 2 respectively. This allows a detailed investigation of the error source providing an insight on how to reduce it. The combined error provides an overall error measure and is calculated using Equation 3. However, the S&G metric is not symmetric and the results vary with the selected baseline curve. To maintain consistency in the current evaluations, the testing curve has been used as the baseline curve $f(t)$ and the simulation curve was $g(t)$ in Equation 2.

Based on the test results [11], it was concluded that the accuracy criteria would only be evaluated for the first load pulse. This was to reduce the effect of reflected tensile waves from the fixture on the load response and that the test was designed such that the first pulse would result in significant damage growth. Figure 6 shows the time interval for which S&G error metric was evaluated for 15 m/s, similar approach was followed for other impact velocities.

$$\text{Magnitude Error} = \sqrt{\frac{I_{gg}}{I_{ff}}} - 1 \qquad (1)$$

$$\text{Phase Error} = \frac{1}{\pi} \times \arccos\left(\frac{I_{fg}}{\sqrt{I_{ff} \times I_{gg}}}\right) \qquad (2)$$

Where

$$I_{ff} = \frac{1}{t_2 - t_1} \times \int_{t_1}^{t_2} f^2(t)dt, \quad I_{gg} = \frac{1}{t_2 - t_1} \times \int_{t_1}^{t_2} g^2(t)dt \quad I_{fg} = \frac{1}{t_2 - t_1} \times \int_{t_1}^{t_2} f(t)g(t)\,dt$$

$$\text{Combined Error} = \sqrt{\text{Magnitude Error}^2 + \text{Phase Error}^2} \qquad (3)$$
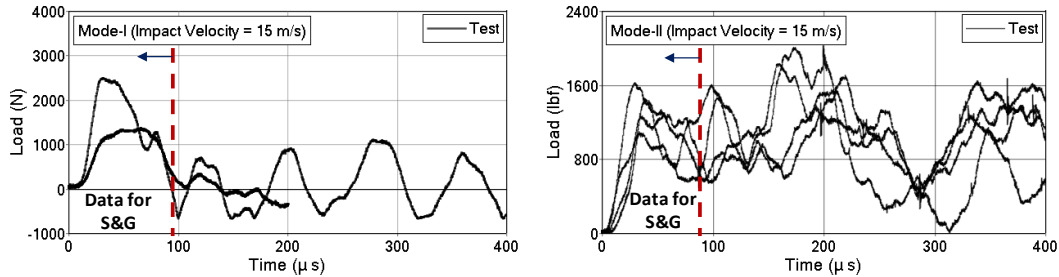

Figure 6 Time interval for evaluation of S&G error metric

Mode-I

Experiments were conducted at quasi-static and dynamic loading rates for Mode-I configuration. It was observed that the primary failure modes were combined cohesive and adhesive failures as shown in Figure 7. MAT162, modeled using orthogonal mesh, predicted adhesive failure and captured plastic deformations in the adhesive bond as shown in Figure 8 . Whereas MAT261, modeled using fiber aligned mesh, predicted both adhesive and cohesive failure as observed in experiments shown in Figure 9 . This could be attributed to fiber aligned mesh ensuring that the energy required to develop the crack is physically correct. It should be noted that similar failure modes were observed for all the dynamic impact velocities.
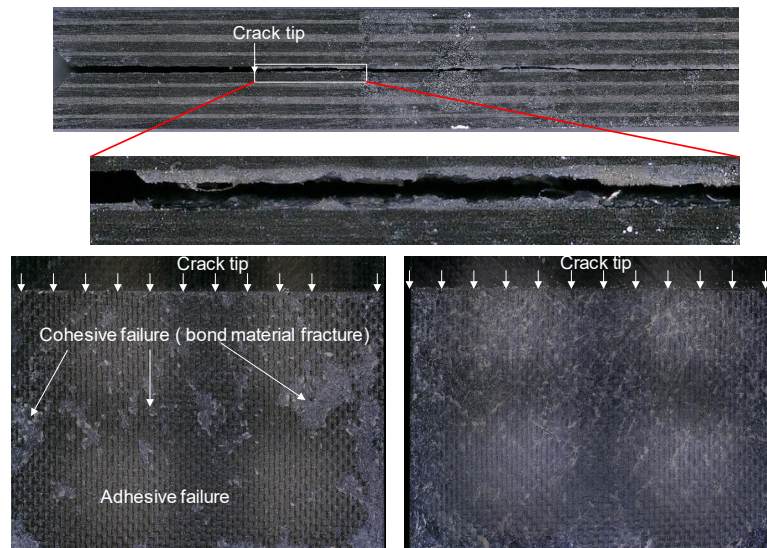
Figure 7 Failure modes observed in Mode-I experiments at 10 m/s [11]
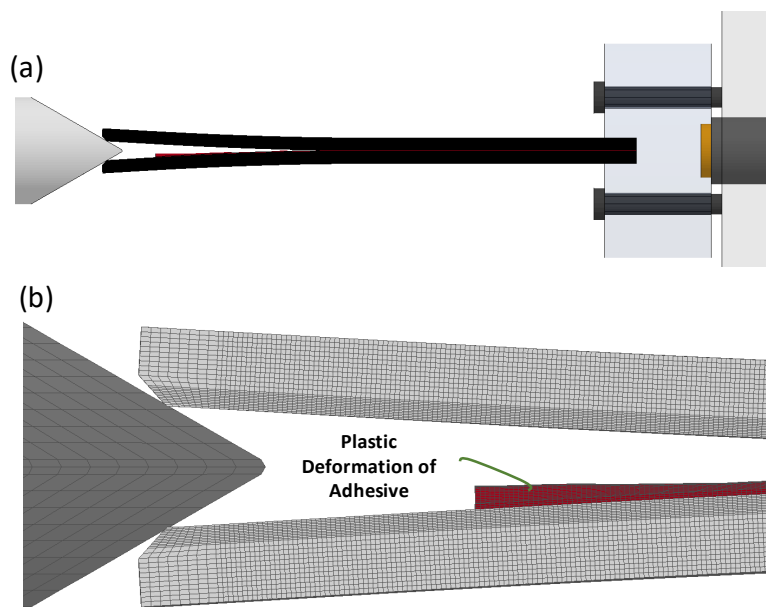

Figure 8 Failure modes observed in Mode-I simulation using MAT 162 (a) Crack propagating at adhesive-composite interface (b) Plastic deformation in adhesive
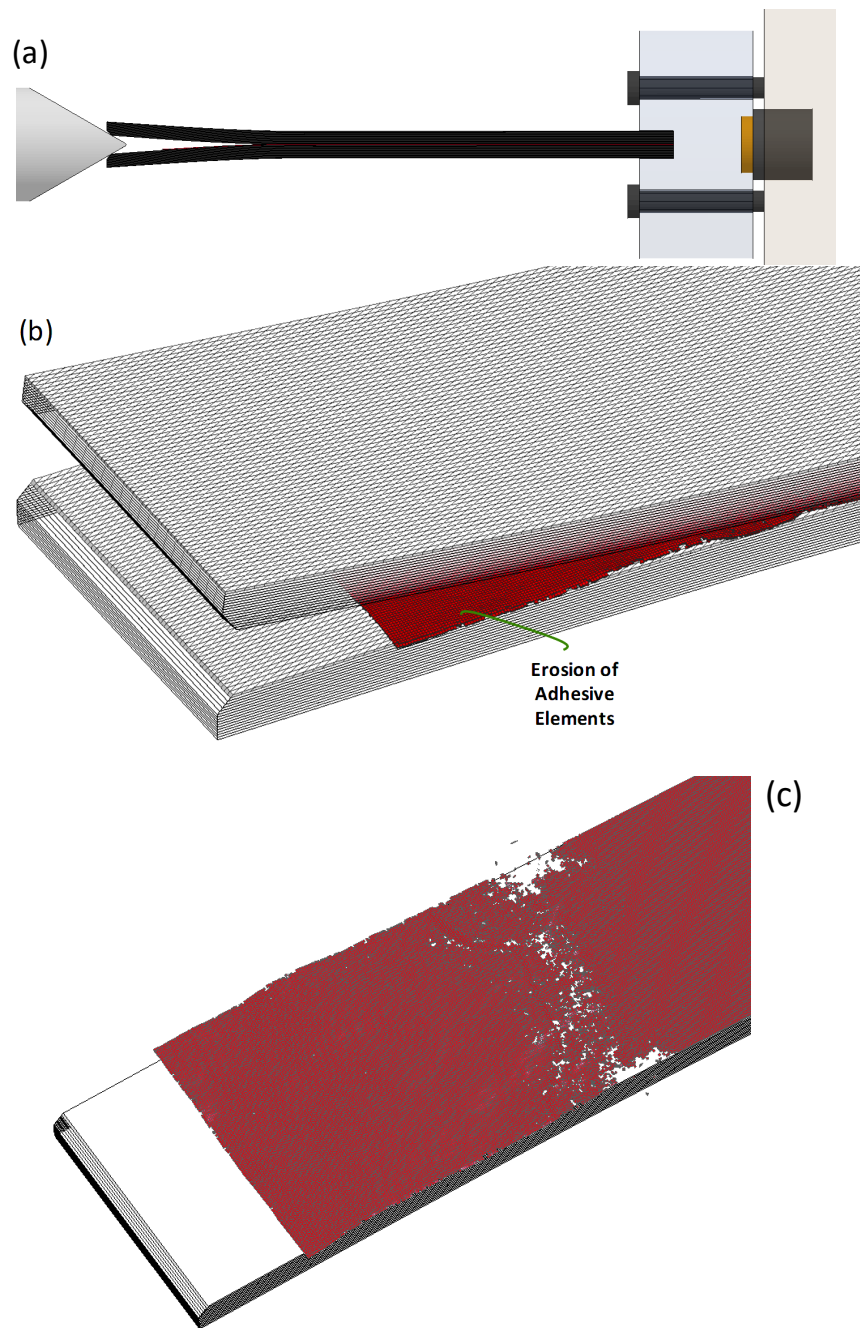
Figure 9 Failure modes observed in Mode-I simulation using MAT261 (a) Crack propagation (b) Plastic deformation and erosion of adhesive (c) Cohesive Failure

A comparison of the global response of load history for both MAT162 and MAT261 has been shown in Figure 10. Simulation results correlated well with experiments for both the material models during the first load pulse (~ 100 μs). Figure 10 also illustrates a comparison of the peak values associated with the first load pulse, between test data and both the material models. The peak loads predicted by both material models exhibit a trend consistent with the test data. However, the predictions are consistently closer to the upper bound of the scatter in the test data. A summary of S&G error metrics has been shown in Figure 11.
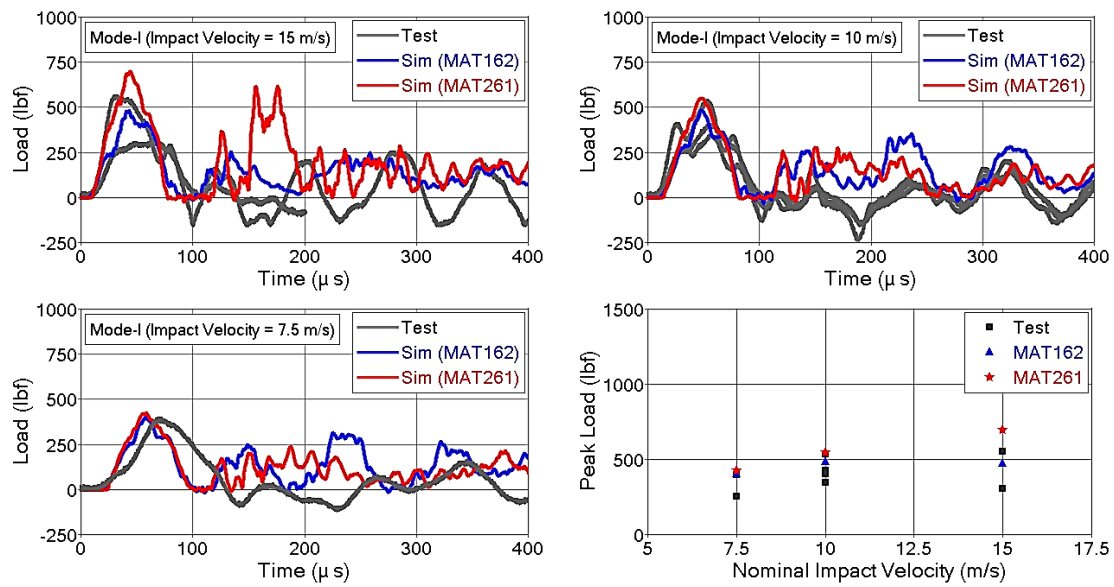
Figure 10 Load response correlation between experiment-analysis for Mode-I
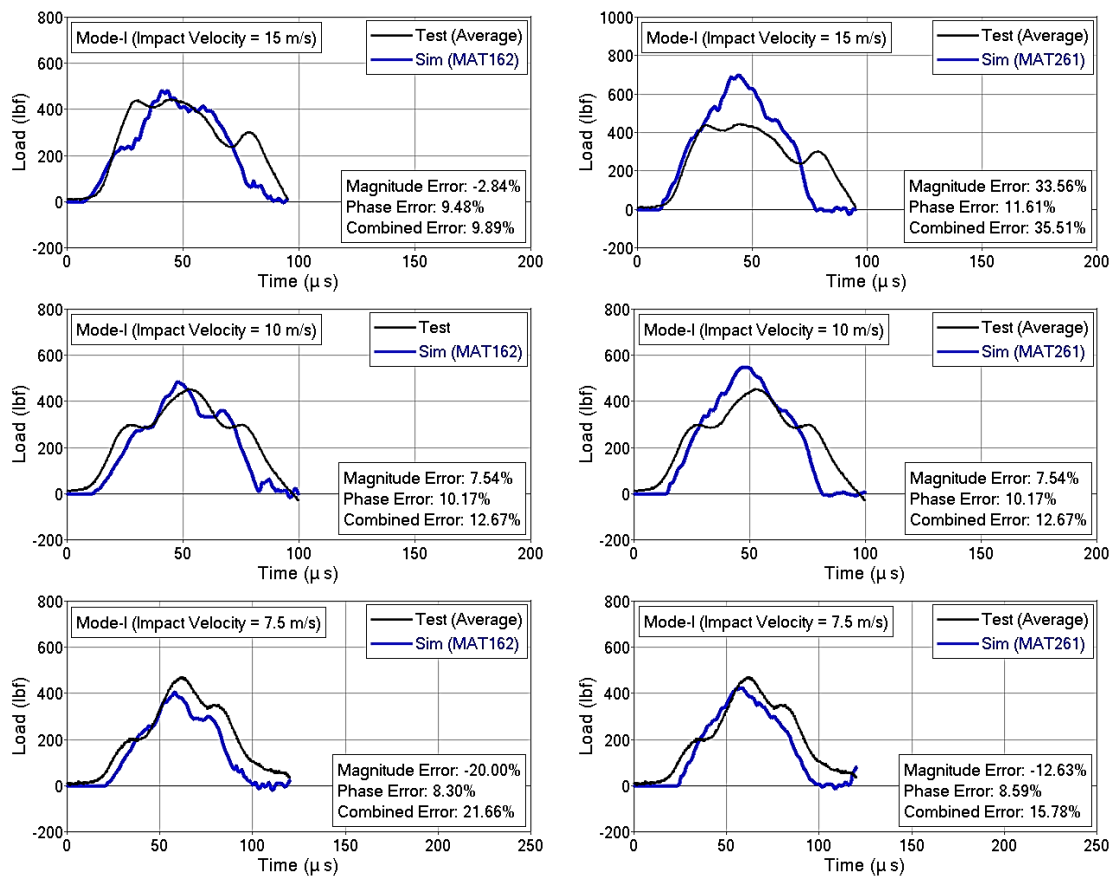

Figure 11 S&G error evaluation for Mode-I test configuration

Mode-II

Experiments were conducted at quasi-static and dynamic impact velocities for Mode-II configuration. It was observed that the crack initiated at adhesive/composite interface and then propagated to composite-composite interface as shown in Figure 12. Delaminations at lower half of laminate were also observed for some specimens, which are possibly an artifact of stress concentrations developed due to ply grouping and free edge effects.

Both material models, MAT162 and MAT261, predicted crack propagation at adhesive/composite interface as shown Figure 13. However, crack migration was not captured due to the modeling methodologies followed.
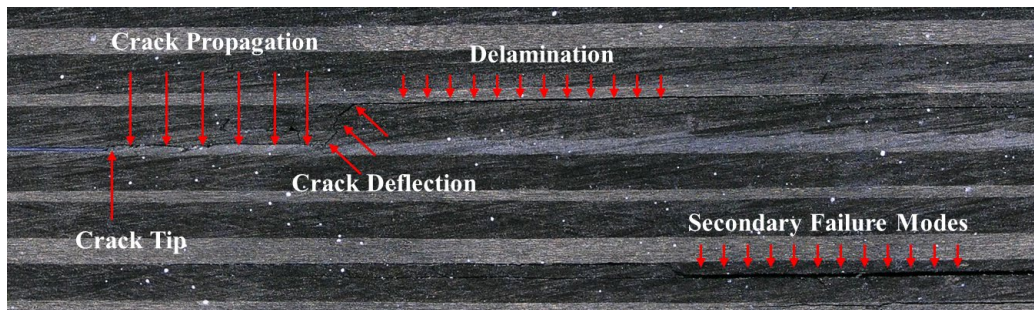

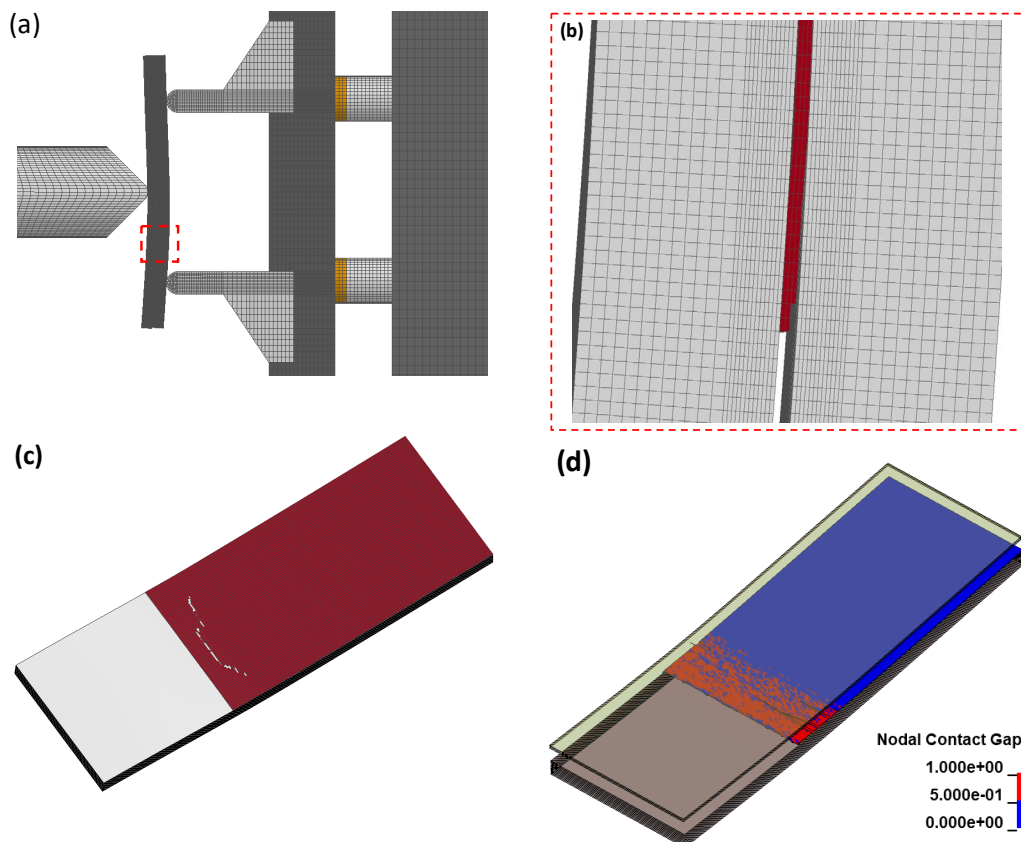Figure 12 Failure modes observed in Mode-II experiments at 7.5 m/s [11]

Figure 13 Failure modes observed in Mode-II simulation for MAT162 and MAT261 (a) Overall kinematics (b) Crack propagation (c) Cohesive failure (d) Nodal gap showing contact release (1=Fail, 0=Not Failed)

A comparison of the global load history response for Mode-II configuration has been shown in Figure 14. Loads obtained from simulation were observed to be greater in magnitude than experimental data for both the material models. A summary of S&G error metrics has been presented in Figure 15.
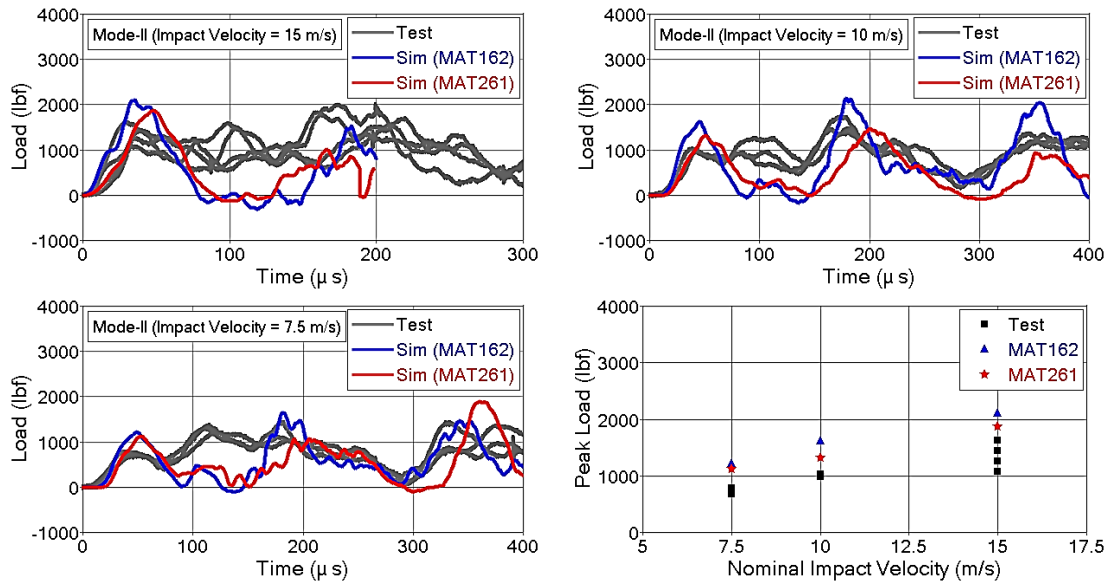

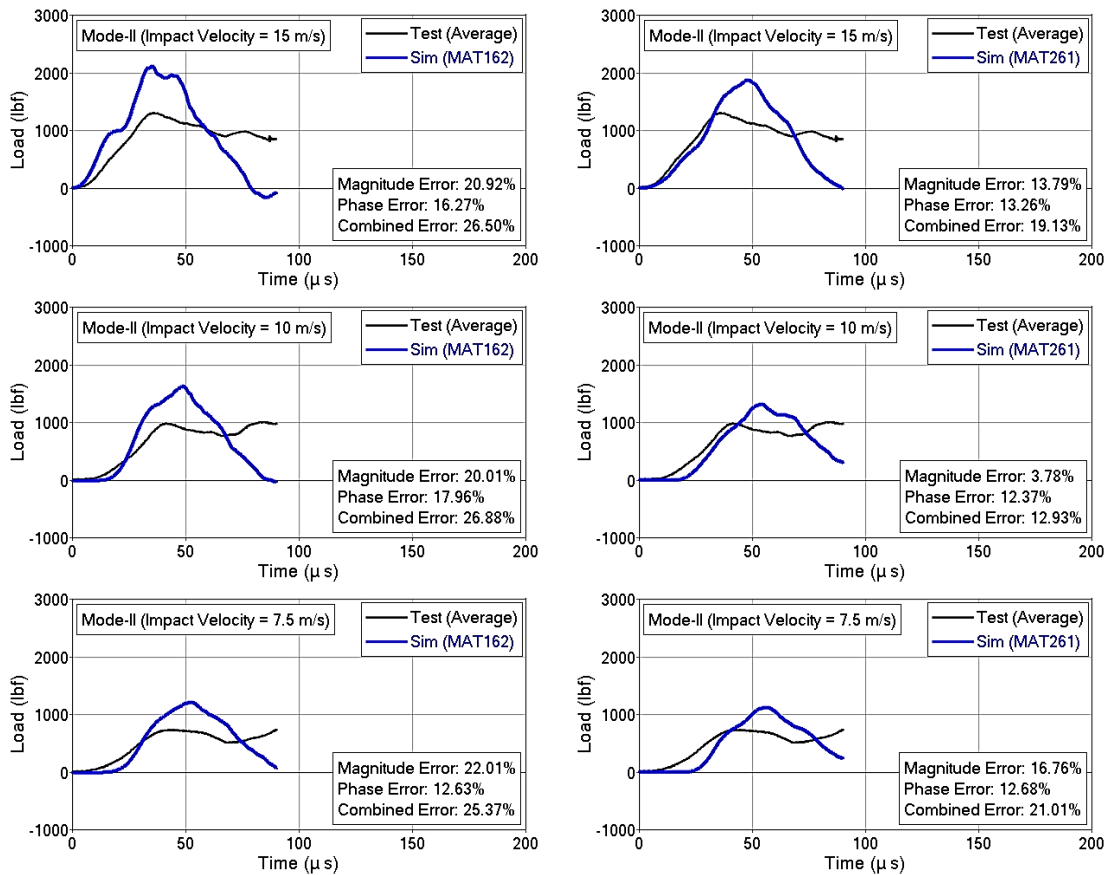Figure 14 Load response correlation between experiment-analysis for Mode-II

Figure 15 S&G error evaluation for Mode-II

CONCLUSIONS

Adhesively bonded CFRP joints subjected to stress pulses generated due to dynamic impact velocities of 7.5 m/s, 10 m/s and 15 m/s were investigated numerically using two commercially available PDFA material models – MAT162 and MAT261. Test-analysis correlation was performed to evaluate simulation capabilities in comparison to experimentally measured load responses while also qualitatively considering modes of failure. Different meshing methodologies were followed – orthogonal mesh for MAT 162 and fiber aligned mesh for MAT 261.

For Mode-I configuration, both MAT162 and MAT261 material models predicted load response which correlated well with the experimental data. MAT162 captured adhesive failure, whereas MAT261 captured both adhesive and cohesive failure similar to the failure modes observed in experiments. This shows that the high fidelity FE model allowed to capture experimental trends correctly and can be used to further investigate different material systems and allow an in-depth understanding of effect of HEDI on fracture behavior of adhesively bonded multi-directional composite laminates.

For Mode-II configuration, both the material models predicted crack initiation at the interface of adhesive/composite, but could not capture crack propagation to composite-composite interface due to limitation of modeling methodologies. Load levels predicted in simulations were higher in comparison to test data. This discrepancy could be attributed to the shear stress parameter required for tiebreak contacts which was calibrated based on fracture toughness value obtained from quasi-static testing. The average apparent fracture toughness value was prominently higher as it was not possible to extract a fracture toughness value for adhesive since the crack migrated to adjacent surfaces due to the wavy nature of FEP insert [9].

ACKNOWLEDGEMENTS

REFERENCES

1. M. Melis, J. M. Pereira, R. Goldberg and M. Rassaian, "Dynamic Impact Testing and Model Development in Support of NASA's Advanced Composites Program," *2018 AIAA/ASCE/AHS/ASC Structures, Structural Dynamics, and Materials Conference, Kissimmee, 2018*.
2. B. Justusson, J. Pang, M. Molitor, M. Rassaian and R. Rosman, "An Overview of the NASA Advanced Composites Consortium High Energy Dynamic Impact Phase II," *AIAA/ASC/ASCE/ Structures Conference*, San Diego, 2019.
3. S. Thorsson, A. Waas, J. Schaefer, B. Justusson and S. Liguore, "Effects of Elevated Loading Rates on Mode I Fracture of Composite Laminates Using a Modified Wedge-Insert-Fracture Method," *Composites Science and Technology,* vol. 156, pp. 39-47, 2018.
4. LS-DYNA*, "Keyword User's Manual-II," 05 December 2017.*
5. *Allen J. Fawcett, Gary D. Oakes, "Boeing Composite Airframe Damage Tolerance and Service Experience"*
6. *J.D. Schaefer, B.T. Werner, I.M. Daniel, "Strain-Rate-Dependent Failure of a Toughened Matrix Composite", Experimental Mechanics, Vol. 54, pp. 1111-1120 ,2014.*
7. S. Ravindran, S. Sockalingam, A. Kidane, M. Sutton, B. Justusson and J. Pang, "High Strain Rate Response of Adhesively Bonded Fiber-Reinforced Composite Joints: A Computational Study to Guide Experimental Design," *Dynamic Behavior of Materials,* pp. 157-162, 2019.
8. The Boeing Company, "Deliverable 5.9.6 Task 7: Material Coupon Characterization Data Analysis and Material Model Calibration", *ACC Phase I HEDI Deliverable Item 5.9.6,* March 6, 2017
9. *The Boeing Company, University of South Carolina, Wichita State University, "2C19 – High Energy Dynamic Impact (HEDI) Deliverable Item 4.9.32 Standard/Non-Standard Coupon Test Report", ACC Phase II HEDI Deliverable item 4.9.32,* May 25, 2019
10. Sprague M.A., Geers T.L., "A spectral-element method for modelling cavitation in transient fluid-structure interaction", *International Journal for Numerical Methods in Engineering*, July 2, 2004
11. The Boeing Company, University of South Carolina, Wichita State University, "2C19 – High Energy Dynamic Impact Deliverable Item 4.9.6 Bonded Joints Test Report", *ACC Phase II HEDI Deliverable item 4.9.6*, August 1, 2019